# Spatiotemporal Wind Energy Potential Assessment Considering Turbine Technology, Power Grid Connectivity, and Land-Use Efficiency

Kwabena A. Kyeremeh, *Graduate Student Member, IEEE,* Rosemary E. Alden, *Member, IEEE,* Aron Patrick, and Dan M. Ionel, *Fellow, IEEE*

***Abstract*—The increasing demand for electricity due to the expansion of data centers necessitates a more integrated and diverse generation mix to improve overall grid reliability and resilience. Wind energy, with its temporal complementarity to solar PV generation, may contribute to meeting this rising demand. A spatiotemporal assessment framework that leverages publicly available datasets to identify technically and spatially suitable sites for wind turbine deployment and energy generation is presented in this study. The framework employs four complementary metrics: capacity factor (CF), and three novel metrics, land-use efficiency (LUE), substation suitability index (SSI), and a composite wind site suitability index (WSSI) to evaluate resource potential, land productivity, and grid accessibility. By aligning wind generation patterns with regional demand variations and grid hosting capacity, renewable deployment can be strategically distributed near emerging data center clusters, thereby reducing transmission losses and enhancing load balancing. A case study of the Commonwealth of Kentucky demonstrates the framework's practical application, integrating wind resource datasets, land cover information, predefined exclusion zones, and existing power grid infrastructure. The results reveal substantial land availability suitable for wind turbine installation and indicate that the Commonwealth possesses sufficient potential to contribute toward meeting its regional annual energy demand, particularly under configurations in which energy storage is expected to complement wind generation.**

***Index Terms*—rid-integrated renewables, land-use efficiency, load dynamics, power system planning, spatiotemporal analysis, hosting capacity, turbine technology, wind energy potential assessment.rid-integrated renewables, land-use efficiency, load dynamics, power system planning, spatiotemporal analysis, hosting capacity, turbine technology, wind energy potential assessment.G**

## I. Introduction

The growing demand for electricity, driven by energy-intensive computing infrastructures, particularly data centers, is reshaping spatial and temporal load profiles. These facilities, often sited based on land availability and access to grid infrastructures, operate at high capacity and require uninterrupted power supply [1]. As their presence expands across the grid, the need for reliable, spatially aligned, and temporally responsive power delivery becomes important in planning frameworks.

Wind energy, characterized by its temporal complementarity to solar generation, may contribute to supporting this rising demand [2]. When strategically integrated, it may diversify the generation mix and enhance grid resilience, particularly when sited near major load centers such as data center clusters. To realize this potential, a detailed understanding of spatial wind resource variability and temporal generation patterns is required. Spatiotemporal assessment frameworks are therefore essential to identify technically suitable and strategically located wind sites that align resource potential with grid accessibility, land availability, and evolving regional demand profiles.

Latinopoulos *et al.* proposed a GIS-based multi-criteria framework for wind farm siting, with limited consideration for temporal demand variability, power operational constraints, and wind resource dynamics [3]. The study by Siyal *et al.*, also presents a GIS-based estimation of onshore wind potential that incorporates environmental and land-use constraints neglecting electricity demand and power grid operational dynamics [4].

Recent advances, including the work by Lopez *et al.*, embed turbine technology, spatial density scaling, and land-use interactions, enhancing the specificity and practicality of capacity assessments [5]. While these advancements have improved the practical relevance of wind energy assessments, many still emphasize static spatial feasibility, neglecting the temporal dynamics of wind resource availability, grid conditions, and evolving demand patterns.

Harrison-Atlas *et al.* advanced localized wind power potential assessment by employing a machine-learning-based framework to generate high-resolution spatial predictions of capacity densities [6]. Similarly, Dai *et al.* proposed a machine learning approach to integrate geospatial analysis in assessing spatial distribution of wind energy capacity potential [7]. The work by Alden *et al.* presented an approach to assess the spatiotemporal capacity potential of DERs with applied EOFs and max-p unsupervised learning techniques to identify zones of similar output power [8]. Considerations for power grid and demand variability constraints are not integrated in the methodologies proposed in these studies.

A GIS-based intuitionistic fuzzy logic is proposed by Sahin *et al.* that provides an uncertainty-aware approach for hybrid solar-wind site selection [9]. Likewise, Demir *et al.* presents

Kwabena A. Kyeremeh, and Dan M. Ionel are with SPARK Lab, Stanley and Karen Pigman College of Engineering, University of Kentucky, Lexington, KY, USA (e-mail: kwabena.kyeremeh@uky.edu; dan.ionel@ieee.org).

Rosemary E. Alden was with the SPARK Lab, Stanley and Karen Pigman College of Engineering, University of Kentucky, Lexington, KY, USA at the time of the work. She is now with ABB Inc. in Raleigh, NC, USA (email: rosemary.alden@ieee.org).

Aron Patrick is with the Research and Development Department, PPL Corporation, Allentown, PA, USA (email: ALPatrick@pplweb.com).


Fig. 1. Experimental setup at the PPL Renewable Energy Integration Research Facility, located at the E.W. Brown Generation Station. The site integrates a utility-scale wind turbine, a 1 MW/2 MWh Battery Energy Storage System, and a utility-scale solar PV array for renewable generation and grid-integration studies. The inset highlights the BESS installation, including the power conversion system, variable load bank, and 13.8kV/480V transformer configuration.

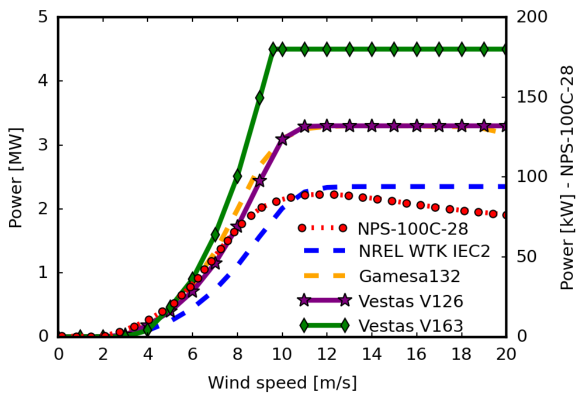


Fig. 2. Wind turbine power–speed curves for low- and high-wind-speed turbines, illustrating how different designs optimize energy capture across varying wind regimes and highlighting the distinct operational characteristics that define each turbine class.

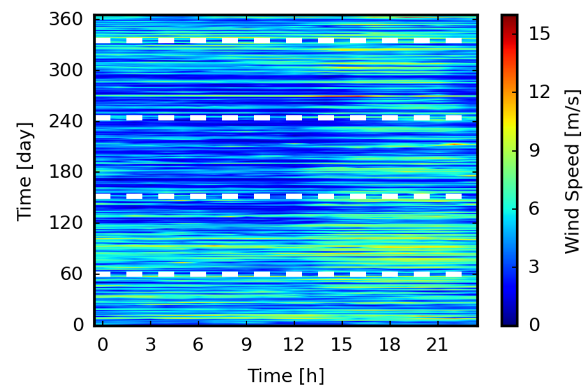


Fig. 3. Yearly wind-speed profile at the experimental site with minutely resolution. Dotted lines mark meteorological seasons, with evening periods showing consistently higher wind speeds.

a GIS-based fuzzy MCDM by integrating F-SWARA and F-MARCOS methods in ranking wind farm locations using environmental and infrastructure factors [10]. Key limitations shared by both are the reliance on static wind speed datasets and expert driven weights to quantify each siting criteria.

Complementary to spatial models, Yu *et al.* proposed a probabilistic methodology by using spatiotemporal quantile regression algorithm in predicting regional wind power [11]. A hybrid spatiotemporal probabilistic framework is presented by Arrieta-Prieto *et al.* that combines temporal modelling with support vector regression and employs DVINE copula to represent spatial dependence [12]. Both probabilistic approaches estimate wind generation independently of power system infrastructure and demand dynamics.

Beyond resource characterization, grid-aligned siting approaches now consider power network integration and demand-driven deployment. Spatial models that incorporate location close to substations, proximity to transmission lines, and load distribution pose more operationally feasible siting options [13]. Planning-level innovations like renewable energy priority zones co-optimize technical feasibility with policy and infrastructure constraints. Such developments suggest a shift from stand-alone resource potential evaluation to system-centric deployment models [14].

Despite significant progress, few studies adequately address the interrelationship of technology advancement, temporal variation of resource and power demand, grid connectivity, and land-use efficiency. Most frameworks are constrained to spatial or temporal domains or simplify transmission considerations to geometric proximity. This gap highlights the need for comprehensive, spatiotemporally resolved frameworks that collectively assess site suitability, resource profiles, grid connectivity, and load dynamics.

This paper advances the spatiotemporal wind energy assessment framework proposed by Kyeremeh *et al.* through three key methodological enhancements [13]. First, a substation suitability index (SSI) is developed to enable grid-aware siting by integrating voltage level as a proxy for hosting capacity and incorporating distance-decay effects to represent interconnection feasibility. Second, a technology- and land-sensitive resource evaluation combines capacity factor (CF) and land-

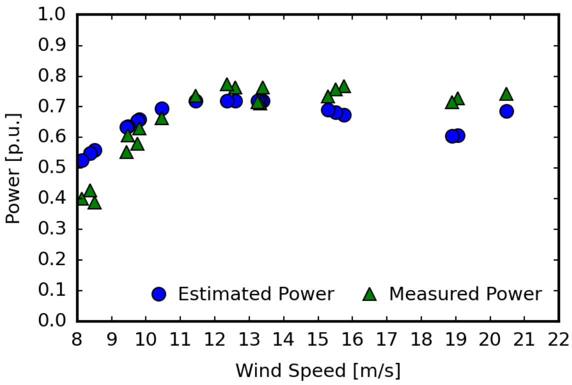


Fig. 4. Example comparison between the measured and estimated power for the experimental wind turbine illustrating the successful validation of computational procedures.

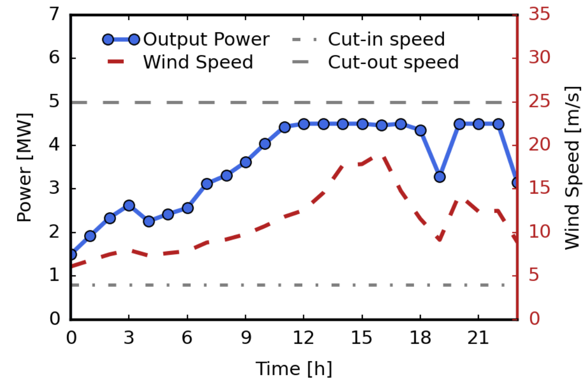


Fig. 6. Example daily power output of the low wind speed Vestas V163 IEC IIIB turbine at the experimental site, illustrating the relationship between measured wind speed and corresponding turbine output power

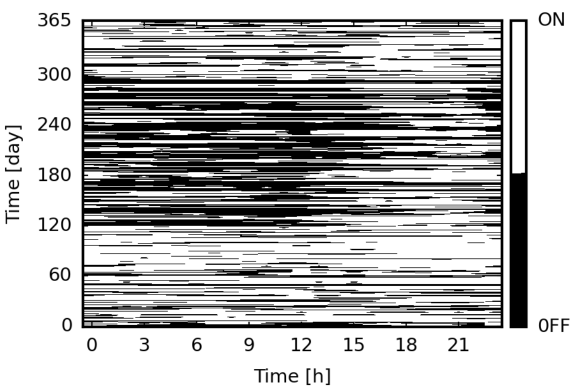


Fig. 5. Status profile of the Vestas V163 at the experimental site, showing ON/OFF operation over daily cycles. White areas indicate turbine operation, while black areas mark downtime. The plot captures seasonal variability and diurnal patterns in turbine availability under site-specific wind conditions.

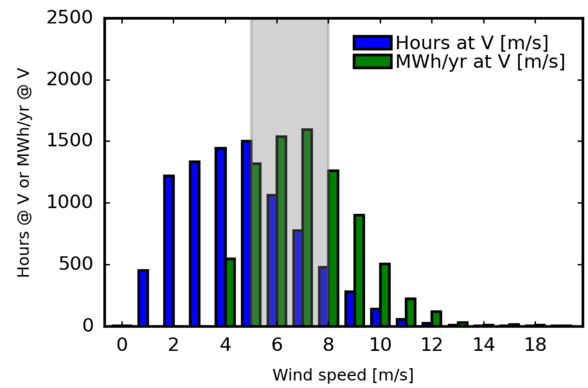


Fig. 7. Distribution of annual wind speed hours and corresponding annual energy generation at the experimental site. The shaded region highlights the effective operating range of the turbine, where maximum energy generation is concentrated.

use efficiency (LUE, GWh/km²) to quantify spatial energy productivity while accounting for turbine performance and land constraints. Third, a composite wind site suitability index (WSSI) aggregates SSI, CF, and LUE within a multi-criteria ranking framework to provide a measure of wind development potential. Collectively, these metrics integrate infrastructure accessibility, turbine technology improvements, and spatial efficiency into a unified spatiotemporal model, establishing a robust decision-support tool for grid-aligned and resource-efficient wind energy planning.

The remainder of this paper is structured as follows. Section II presents the experimental setup and site-specific wind energy potential assessment, describing the study site, turbine specifications, and data used for the analysis. Section III introduces the analytical framework for evaluation of wind site suitability, specifying the data sources, preprocessing steps, exclusion scenarios, and the definitions of evaluation metrics. Section IV provides experimental validation through a case study estimating grid-integrated potential of wind energy in the Commonwealth of Kentucky, USA. Section V discusses the results, insights, and implications for planning and policy. Finally, Section VI concludes the paper by summarizing the key findings and describing potential areas for future studies.

## II. Experimental Setup and Site-Specific Wind Energy Potential Assessment

The PPL Renewable Integration Research Facility (Fig. 1) at the E.W. Brown Generation Station serves as the experimental platform for this study. The site comprises a utility-scale solar photovoltaic (PV) array, a 1MW/2MWh lithium-ion battery energy storage system (BESS), a wind turbine, and an integrated weather monitoring station. This hybrid renewable testbed offers a unique environment for assessing site-specific wind energy potential and analyzing the operational dynamics of multi-source renewable grid integration.

The experimental utility-scale wind turbine installed at the E.W. Brown site is a Northern Power Systems NPS 100C-27, a 100kW permanent-magnet direct-drive machine, which features a 27.4m rotor diameter, 36.6m hub height, and an upwind three-blade configuration compliant with IEC 61400-1 Class S standards. The turbine operates with variable-speed stall control, cutting in at approximately 2.5m/s and rated at 11m/s, with a cut-out of 20m/s as shown in Fig 2.

The wind speed, illustrated in Fig. 3, was measured using a precision and accurate anemometer placed at a standard height of 10m [15]. The data was then scaled, using well established procedures including equation in (1), for the hub

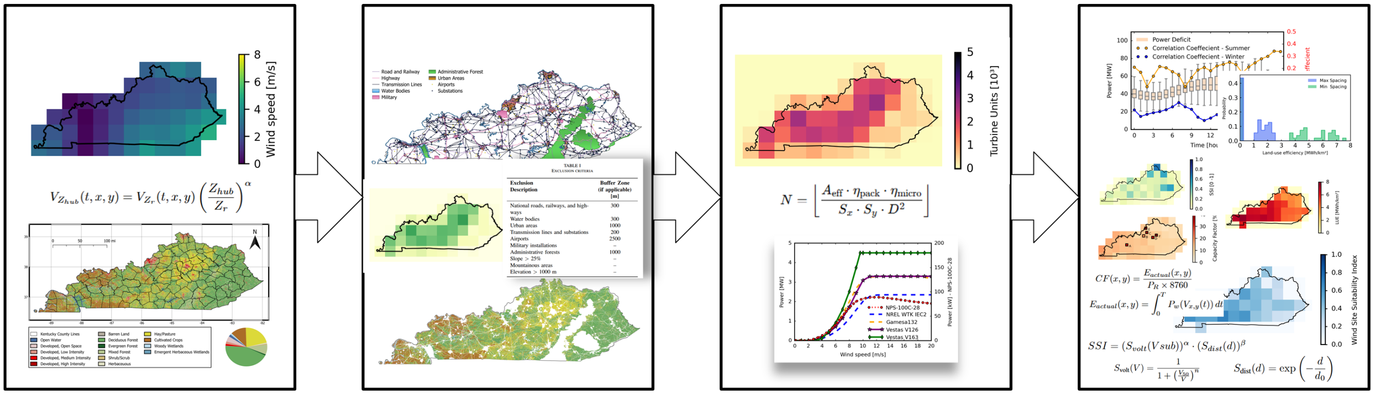


(a) (b) (c) (d)

Fig. 8. Framework for the spatiotemporal wind energy potential assessment. The workflow includes (a) data collection and wind speed scaling using terrain information from the land cover dataset, (b) application of land-use and grid infrastructure exclusions, (c) turbine siting and energy estimation, and (d) development of novel composite metrics and spatial evaluation through the Wind Site Suitability Index.

height corresponding to the NPS 100C existing experimental prototype and to the large scale Vestas V163-4.5MW (IEC IIIB) proposed turbine, respectively as described in [16]:

$$V_{Z_{hub}}(t) = V_{Z_r}(t)\left(\frac{Z_{hub}}{Z_r}\right)^{\alpha}, \tag{1}$$

where $V_{Z_{hub}}$ is the wind velocity at turbine hub height, $Z_{hub}$, and $V_{Z_r}$ the velocity at the reference measurement height. The surface roughness coefficient, denoted as $\alpha$, is assigned a value of 0.15 to represent the prevailing land cover characteristics at the research facility site [17]. The data for the wind speed and electric power for the existing experimental wind turbine was also used to validate the computational procedures, achieving a satisfactory range of $+/-10\%$, as illustrated in Fig. 4.

The annual status profile, shown in Fig. 5, illustrates the V163 turbine ON/OFF operation governed primarily by the availability of adequate wind speeds. Continuous operation occurs when wind velocities lie within the turbine's designed range, while downtime may result from wind speeds falling below the cut-in threshold or exceeding the cut-out limit. This temporal variability may indicate the diurnal and seasonal fluctuations characteristic of low-wind-speed environments.

An example daily wind speed profile and corresponding power output are shown in Fig. 6. The observed consistency between wind variations and power response suggests that the turbine could operate optimally within its intended design envelope under the site's wind conditions.

The distribution of annual wind speed hours and corresponding energy generation is shown in Fig. 7. The shaded region represents the effective operating range of the turbine, where the highest frequency of wind speed occurrences and maximum energy yield are concentrated. This alignment between the available wind resource and turbine efficiency indicates that the V163 turbine may be suitably matched to the site.

## III. Analytical Framework for Spatiotemporal Wind Energy Evaluation

This section presents a regional-level spatiotemporal assessment of wind energy potential, incorporating spatial variability, temporal dynamics of wind speed, and the availability of existing grid infrastructure. The overall methodological framework guiding this assessment is summarized in the flowchart provided in Fig. 8. Hourly wind data with a spatial resolution of 50km x 50km at an altitude of 50m shown in Fig. 9(a), was obtained from the open source NASA Earthdata Pathfinder MERRA-2 reanalysis climate dataset [18]. MERRA-2 was selected because it provides a climate-consistent, multi-decadal atmospheric record generated using a stable data assimilation framework that reduces spurious trends associated with changes in observing systems [19].

A 50km × 50km resolution is considered sufficient for the objectives of this study, which emphasize regional-scale spatiotemporal assessment and planning-level analysis rather than site-specific micro-siting. At this scale, dominant atmospheric drivers of wind variability are adequately captured, and finer spatial resolution may not affect regional patterns or planning-relevant conclusions.

The availability of land suitable for wind farm deployment, which is primarily determined by land use characteristics, is a critical factor in wind energy development [20]. This study employs land cover data from the National Land Cover Database (NLCD), illustrated in Fig. 9(b), which provides classifications at a 30m × 30m resolution [21].

To identify suitable locations for turbine siting, specific land cover types and infrastructure elements were excluded based on environmental, regulatory, and industry criteria. Excluded areas include water bodies, roads, highways, railways, protected forests, airports, urban zones, transmission lines, and electrical substations. Buffer zones were applied around these features to account for safety requirements and standard siting practices, as shown in Fig. 10(a). The spatial application of the exclusion criteria yields the available land illustrated in Fig. 10(b).

It is essential to consider turbine array spacing when estimating the number of turbines deployable on an available land, as improper layout may increase wake losses and structural fatigue [16]. The spacing formulation originally presented in [17] is modified in this study to incorporate additional cor-

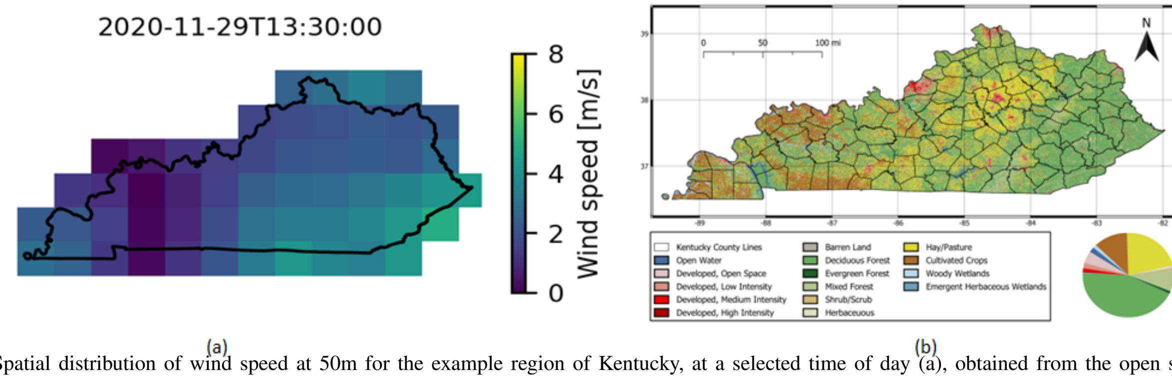


Fig. 9. Spatial distribution of wind speed at 50m for the example region of Kentucky, at a selected time of day (a), obtained from the open source NASA EarthData Pathfinder dataset. The land-use and land-cover classifications (b), from the National Land Cover Data, is presented with the accompanying pie chart summarizing the relative share of each category. Together, these maps illustrate the spatial variability of wind resources and land use constraints relevant to wind energy assessment.

rection parameters accounting for practical siting constraints:

$$N = \left[ \frac{A_{\text{eff}} \cdot \eta_{\text{pack}} \cdot \eta_{\text{micro}}}{S_x \cdot S_y \cdot D^2} \right], \tag{2}$$

where $A_{\text{eff}}$ is the exclusion-adjusted parcel area, $S_x$ and $S_y$ the spacing multipliers within and between rows, respectively, $D$ the rotor diameter, $\eta_{\text{pack}}$ accounts for geometric inefficiencies due to irregular land shapes, and $\eta_{\text{micro}}$ corrects for practical siting constraints such as roads and maintenance access. As previously discussed, the turbine power–speed curve relationship is applied to estimate the annual wind energy production of individual turbines across grid cells defined by latitude (x) and longitude (y), as [17]:

$$E_{\text{actual}}(x, y) = \int_0^T P_w(V_{x,y}(t))dt, \tag{3}$$

where $E_{\text{actual}}(x, y)$ represents the energy output of a single turbine within a grid cell, $T$ is the observation duration, and $P_w(V_{x,y}(t))$ denotes the turbine power as a function of time-varying wind speed. Owing to temporal variations in wind velocity, the actual energy yield constitutes a fraction of the theoretical maximum output, expressed as the capacity factor [17], and computed as:

$$CF(x, y) = \frac{E_{actual}(x, y)}{P_R \times 8760}, \tag{4}$$

where $CF(x, y)$ is the capacity factor of a grid cell, $E_{actual}$ the actual energy delivered in the considered grid cell, and $P_R$ the turbine's rated power. To complement the temporal assessment provided by the capacity factor, land-use efficiency is used to evaluate the spatial efficiency of candidate wind energy sites. LUE quantifies the annual energy generated per unit area of land occupied by turbines and is defined as:

$$LUE(x, y) = \frac{E_{\text{actual}}(x, y)}{A_{\text{turbine}}}, \tag{5}$$

where $LUE(x, y)$ is the land-use efficiency of a grid cell and $A_{\text{turbine}}$ the area allocated per turbine.

The viability of a wind site depends not only on resource availability and turbine technology but also on the feasibility of power grid interconnection. To capture this grid-related dimension of site assessment, a substation suitability index (SSI) is introduced, which is quantified through a composite index that reflects both the technical compatibility of a substation and its spatial accessibility.

This metric is expressed as a weighted product of substation capacity and distance suitability terms:

$$SSI = (S_{cap}(Vsub))^{\alpha} \cdot (S_{dist}(d))^{\beta}, \tag{6}$$

where $S_{cap}(Vsub)$ quantifies the adequacy of the substation's voltage rating $V_{sub}$ for large-scale integration serving as a proxy for transformer capacity and overall grid hosting strength. In the absence of publicly available transformer ratings, nominal voltage may serve as a reliable indicator of the substation's inherent ability to accommodate high-power injections, as higher-voltage substations are typically designed for greater power transfer capacity [22], [23]. $S_{dist}(d)$ represents the penalty associated with the geographic distance $d$, between the substation and the wind site. The exponents $\alpha$ and $\beta$ serve as weighting factors that reflect the relative importance of voltage strength versus distance minimization in a given planning context.

The capacity suitability score is modeled using Hill's function, a type of Sigmoidal function, that increases monotonically with voltage [24]:

$$S_{\text{cap}}(V) = \frac{1}{1 + \left(\frac{V_{50}}{V}\right)^n}, \tag{7}$$

where $V_{50}$ represents the characteristic voltage at which suitability is 0.5, and $n$ controls the steepness of the transition. This formulation ensures that substation suitability rises rapidly as voltage exceeds the mid-capacity threshold but gradually saturates for very high voltages.

The distance suitability reflects the decline in feasibility as the transmission lines lengthens, modeled with an exponential decay:

$$S_{\text{dist}}(d) = \exp\left(-\frac{d}{d_0}\right), \tag{8}$$

where $d_0$ is a characteristic decay parameter. Smaller $d_0$ values penalize distance more severely, reflecting planning contexts where interconnection costs are highly sensitive to transmission line length.

A composite wind site suitability index is proposed to

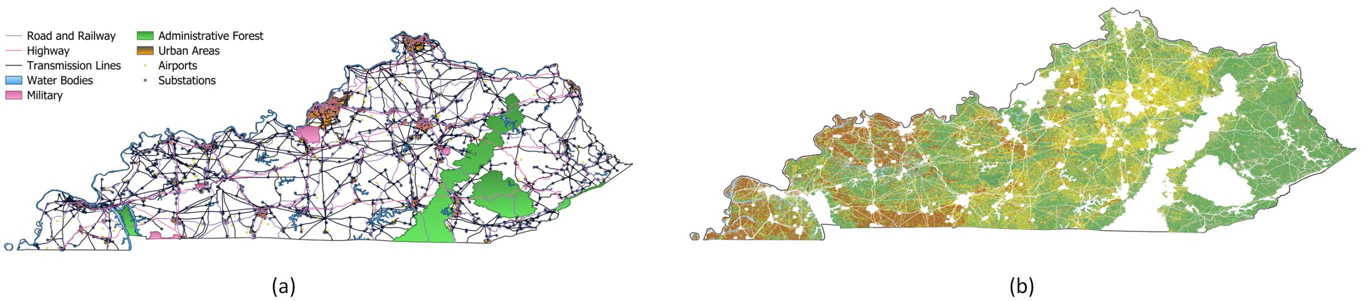


Fig. 10. Land cover types and facilities excluded from the land cover data (a), in evaluating suitable land for wind turbine deployment. Spatial application of these exclusion criteria (b) across the study region demonstrates the reduction in available land. Suitable land for wind turbine siting after application of the exclusions is about $77 \times 10^3$ km$^2$ , which is approximately 73% of the region's total land area.

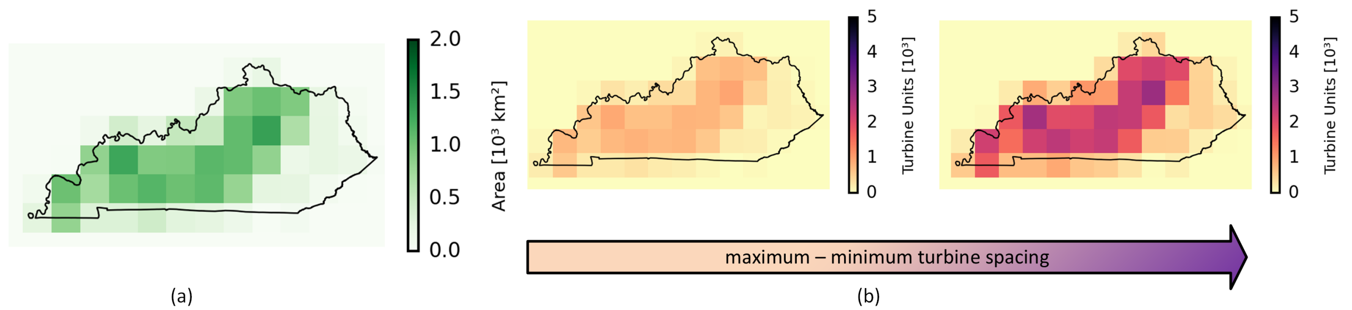


Fig. 11. Spatial distribution of (a) available land area for turbine deployment after applying siting exclusions, and (b) estimated turbine units per grid cell under maximum (left) and minimum (right) spacing configurations. The difference between spacing scenarios is highlighted by the color gradient, with minimum spacing allowing significantly higher turbine density across much of the state.

TABLE I
SUMMARY OF SITING EXCLUSION CRITERIA AND BUFFER DISTANCES

| **Exclusion Description** | **Buffer Zone (if applicable) [m]** |
|---|---|
| National roads, railways, and highways | 300 |
| Water bodies | 300 |
| Urban areas | 1000 |
| Transmission lines and substations | 200 |
| Airports | 2500 |
| Military installations | – |
| Administrative forests | 1000 |
| Slope > 25% | – |
| Mountainous areas | – |

provide an integrated metric for assessing the overall suitability of potential wind energy sites. The index combines three dimensions of performance: turbine output, land-use efficiency, and grid accessibility, into a single quantitative measure. It is expressed as a multiplicative aggregation of three normalized indicators, capacity factor, land-use efficiency, and substation suitability index, expressed as:

$$\mathrm{WSSI} = CF_n^{w_{\mathrm{CF}}} \times LUE_n^{w_{\mathrm{LUE}}} \times SSI_n^{w_{\mathrm{SSI}}} \tag{9}$$

where $CF_n$, $LUE_n$, and $SSI_n$ denote the normalized capacity factor, land-use efficiency, and substation suitability index, respectively, and the non-negative weights $w_{\mathrm{CF}}$, $w_{\mathrm{LUE}}$, and $w_{\mathrm{SSI}}$ sum up to unity.

The CF and SSI indicators are inherently normalized by design in equations (4) and (6)-(8). In contrast, LUE is normalized using a percentile-based min-max transmformation expressed as:

$$LUE_n = \frac{LUE - P_5}{P_{95} - P_5}, \tag{10}$$

where $P_5$ and $P_{95}$ denote the 5th and 95th percentiles of the LUE distribution across all grid cells.

Following normalization, the weighted aggregation is applied across grid cells, using weights selected for this case study to reflect transmission-level planning considerations, with greater emphasis placed on resource adequacy, followed by grid accessibility, and then spatial efficiency. These values remain bounded with [0-1] and are ranked in descending order, with higher WSSI indicating greater overall site suitability.

The matching of wind power generation and electric network loading may serve as an indicator of the need for an energy storage system [25]. The Pearson correlation coefficient is employed in this work to quantify load matching, i.e. the capacity of wind energy generation to meet demand, and is estimated as [26]:

$$A = T\sum_{t=1}^{T}(P_{wt}P_{Lt}) - \left(\sum_{t=1}^{T}P_{wt}\right)\left(\sum_{t=1}^{T}P_{Lt}\right), \tag{11}$$

$$B = \left[T\sum_{t=1}^{T}P_{wt}^2 - \left(\sum_{t=1}^{T}P_{wt}\right)^2\right]\left[T\sum_{t=1}^{T}P_{Lt}^2 - \left(\sum_{t=1}^{T}P_{Lt}\right)^2\right], \tag{12}$$

$$LM = \frac{A}{\sqrt{B}}, \tag{13}$$

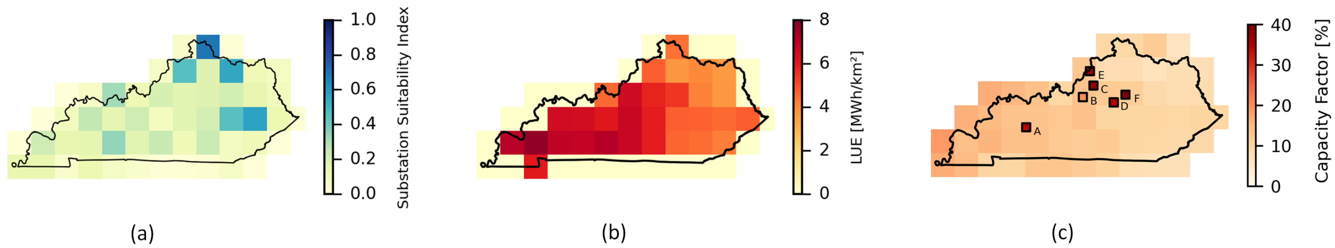


Fig. 12. Spatial distribution of (a) Substation Suitability Index (SSI), (b) Land-Use Efficiency (LUE), and (c) Capacity Factor for the Vestas V163 (IEC IIIb) turbine across Kentucky. Distinct spatial patterns of grid accessibility and land productivity are observed, while (c) shows variations in regional wind potential with both grid-based and point-specific capacity factors from weather stations A–F.

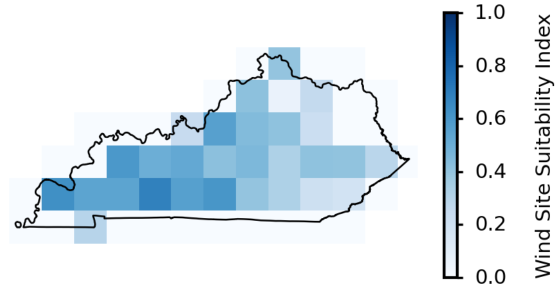


Fig. 13. Wind Site Suitability Index, with 1 being the highest suitability, across Kentucky, combining substation suitability, land-use efficiency, and capacity factor to identify regions where grid accessibility, land availability, and wind resource potential align for optimal turbine deployment.

where $LM$ is the load matching metric, $T$ the timespan, $P_w$ the generated wind power, and $P_L$ the demand. Regional energy storage requirements may be estimated from the wind potential assessment by analyzing annual supply-demand imbalances. The power deficit and excess generation for the study region are quantified through systematic evaluation of the temporal mismatch between wind availability and electricity demand, formulated as:

$$P_{IM} = \begin{cases} \text{deficit} & \text{if } P_L - P_w > 0 \\ \text{excess} & \text{if } P_L - P_w < 0, \end{cases} \tag{14}$$

where $P_{IM}$ is the power imbalance, $P_L$ the demand, and $P_w$ the generated wind power.

## IV. Case Study: Assessing Wind Energy Potential in Kentucky, USA

The proposed wind energy assessment framework is applied to the Commonwealth of Kentucky to evaluate the state's wind resource potential, land-use suitability, and grid accessibility for prospective wind energy development. Barren land, shrub/scrub, herbaceous, hay/pasture, and cultivated crops were chosen as suitable land cover types for onshore wind deployment, as per the criteria detailed in [27].

Buffer zones were applied to exclude areas unsuitable for wind turbine installation, including national roads, railways, highways, water bodies, urban and built-up areas, transmission lines, substations, airports, and administrative forests. In addition to these, areas such as military installations, steep slopes greater than 25%, and mountainous regions are excluded.

The corresponding buffer distances for each exclusion category are summarized in Table I. These setback values were chosen within ranges reported by relevant regulatory and standards bodies, as well as those reported in regional siting assessment studies in the literature [5], [28], [29]. These exclusions are applied to the publicly available land cover dataset, resulting in approximately 73% of Kentucky's total land area remaining available for potential wind energy development, as illustrated in Figs. 10(b) and 11(a).

Within this case study, the 4MW Vestas V163 turbine, designed for low-wind-speed applications in accordance with IEC standards, was selected with a hub height of 140m. The area required per turbine was determined using a rectangular array configuration as described in (2). Two spacing scenarios were evaluated: $((S_x, S_y) = (3, 5))$ and $((S_x, S_y) = (5, 9))$, corresponding to the minimum and maximum turbine spacing configurations [17]. To account for geometric inefficiencies and practical siting needs, additional factors of 0.95 and 0.9 were applied to the available land after exclusions. As shown in Fig. 11(b), the minimum spacing configuration accommodates significantly more turbines across the available land and was therefore adopted for subsequent analyses.

The spatial variation of substation suitability and land-use efficiency is presented in Fig. 12(a) and (b), respectively. As illustrated, higher substation suitability scores are concentrated in the northern regions of the state, which indicate enhanced grid integration potential and may be due to the presence of adequate grid infrastructure. High land-use efficiency values, shown in Fig. 12(b), occur primarily in southwestern regions, where large, contiguous land parcels remain available after applying exclusion criteria and where wind conditions may support efficient turbine deployment.

The spatial distribution of capacity factors across grid cells for the spatiotemporal analysis and the site-specific values estimated from six weather stations [15], are presented in Fig. 12(c). The site-specific estimation, suited for micro turbine siting, present higher values - ranging from about 20% to 40%.

The limited spatial overlap between high land-use efficiency and high substation suitability areas, along with spatial variability in capacity factors, highlights the value of applying the previously defined WSSI. As shown in Fig. 13, the index captures the trade-offs among these dimensions, guiding planners toward regions that offer a balanced potential for wind energy development across the state.

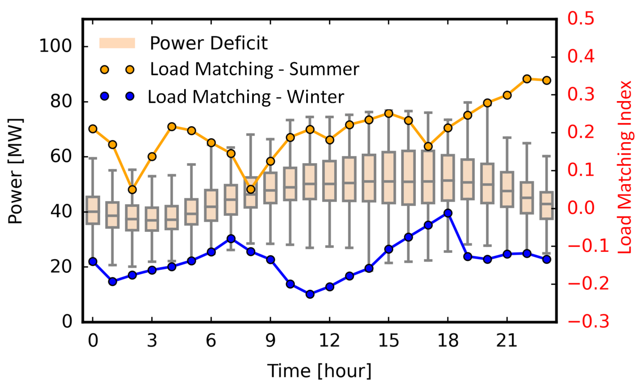


Fig. 14. Seasonal load matching of wind power generation within the grid cell with the maximum generation. The variability and range of power deficits, depicting magnitudes and instances of supply imbalances, are also shown.

Power imbalance and load matching of wind turbine generation for the considered region is illustrated in Fig. 14. For use with the described procedure, aggregated publicly available hourly demand data, obtained from the U.S. Energy Information Administration [30], was disaggregated based on the population density of each defined grid cell. The hourly power deficit, which is the difference between generated wind power and system load, identifies peak imbalances and critical periods of the day needing grid stability management by system operators.

Load matching index across seasons, reveals important insights into how wind energy generation can effectively match the variation in demand throughout the year. Alternate sources like energy storage systems can be employed by utilities to store or deliver energy during mismatch periods.

For the example region, a moderate matching was found for both seasons and across the day, the strongest occurring at night times during the summer. Night-time wind generation at this location serves to complement solar PV output that is mostly available during the day to meet load or charge energy storage systems after high imbalances in the evening.

## V. Discussion

The rapid expansion of data centers, with their high and continuous energy demands, underscores the need for a reliable and diversified energy mix. Wind energy, particularly when integrated with solar PV, offers a complementary and geographically distributable solution that enhances grid reliability and flexibility [2], [31]. By aligning spatiotemporal wind assessments with regional demand and grid hosting capacity, renewable deployment can be strategically distributed near data center clusters, which may reduce transmission losses and improve load balancing.

Accurate estimation of wind energy generation potential becomes essential, not only for power system planning but also for informing utility investment decisions and state-level policy formulation [32], [33]. Spatiotemporal assessment frameworks, such as the one presented in this study, may enable the identification of technically viable sites for wind turbine deployment, especially in regions classified as low-wind-speed zones.

The potential for wind energy generation is inherently determined by the combination of natural resources, i.e. adequate wind speeds and suitable land, and the availability of wind turbine technology. Recent advancements in wind turbine design, particularly the introduction of large rotor diameter and high tip height turbines, significantly enhance efficient energy generation in low and very low wind speed areas. These technological developments have increased wind energy generation potential across regions previously considered unsuitable for such installations [34]–[37].

In applying the proposed method in this paper to other regions, turbine selection should be guided by the corresponding international wind classification standards, ensuring that the chosen turbine aligns with the region's characteristic wind speed class [38]. The Delta Wind project, with about 40 Vestas V150 low wind speed turbines, sited in Mississippi - a low wind speed region, exemplifies recent expansion of wind energy developments [39].

To support wind energy integration, a robust power system grid, with sufficient substation and transmission capacity, is important [40]. The spatial alignment between high-quality wind resource zones and existing grid infrastructure strongly influences the cost-effectiveness of new projects. In addition to technical considerations, national and local regulations on wind turbine siting, designed to address issues including, land use policies, environmental impact, noise restrictions, flight zones, access to restricted areas, and visual impact, must be adhered to.

Incorporating high-resolution spatial and temporal electricity demand may improve the alignment of wind generation characteristics with dynamic load profiles and transmission network constraints. This study represents an ongoing research that includes the integration of high resolution load data and extends the proposed framework through geospatial optimization to identify suitable sites for the co-location of data centers and wind energy resources.

## VI. Conclusion

This study presented a spatiotemporal framework for assessing wind energy potential using publicly available datasets to identify technically and spatially suitable sites for wind turbine deployment. The framework integrates four complementary metrics: capacity factor (CF), land-use efficiency (LUE), substation suitability index (SSI), and the composite wind site suitability index (WSSI) to jointly evaluate resource potential, spatial productivity, and grid accessibility.

By aligning wind generation patterns with regional demand variations and substation hosting capacity, the framework enables strategic placement of renewable generation near emerging high-power-intensive loads, such as data center clusters, thereby reducing transmission losses and improving system load balancing. Seasonal analysis of wind power generation and electrical demand further highlights the potential for generation–demand complementarity across different time scales. Site-specific assessments, based on high-resolution meteorological station data, enable quantification of localized wind resource variability and informing turbine selection.

The proposed framework provides policymakers, utilities, and developers with a practical and data-driven decision-support tool for guiding wind power investment and integration strategies. Application of the framework to a regional case study in Kentucky demonstrates its ability to quantify suitable land availability for wind turbine deployment and estimate its contribution toward meeting annual energy demand. These findings underscore the framework's value in advancing grid-aware, land-efficient, and demand-responsive renewable energy planning, particularly for low-wind-speed regions.

## ACKNOWLEDGMENT

The support of PPL Corporation Research and Development, the National Science Foundation (NSF) under NSF Graduate Research Fellowship Grant No. 2239063, the University of Kentucky L. Stanley Pigman Chair in Power endowment, and of the Lighthouse Beacon Foundation is gratefully acknowledged. Any findings and conclusions expressed herein are those of the authors and do not necessarily reflect the views of the sponsor organizations.

## REFERENCES

[1] A. Shehabi, S. J. Smith, A. Hubbard, A. Newkirk, N. Lei, M. A. B. Siddik, B. Holecek, J. Koomey, E. Masanet, and D. Sartor, "2024 United States Data Center Energy Usage Report," Lawrence Berkeley National Laboratory, Berkeley, CA, USA, Tech. Rep. LBNL-2001637, Dec. 2024.

[2] F. Blaabjerg and D. M. Ionel, *Renewable energy devices and systems with simulations in MATLAB® and ANSYS®*. Boca Raton, FL: CRC Press, 2017.

[3] D. Latinopoulos and K. Kechagia, "A GIS-based multi-criteria evaluation for wind farm site selection. A regional scale application," *Renewable Energy*, vol. 78, pp. 550–560, 2015.

[4] S. H. Siyal, U. Mörtberg, D. Mentis, M. Welsch, I. Babelon, and M. Howells, "Wind energy assessment considering geographic and environmental restrictions: A gis-based approach," *Energy*, vol. 83, pp. 447–461, 2015.

[5] A. Lopez, T. Mai, E. Lantz, D. Harrison-Atlas, T. Williams, and G. Maclaurin, "Land use and turbine technology influences on wind potential in the United States," *Energy*, vol. 223, p. 120044, 2021.

[6] D. Harrison-Atlas, A. Lopez, E. Lantz, T. Williams, G. Maclaurin, and T. Mai, "Spatially-explicit prediction of capacity density advances real-world characterization of onshore wind potential," *Energies*, vol. 14, no. 12, p. 3609, 2021.

[7] T. Dai and C. D. Scown, "A novel approach for large-scale wind energy potential assessment," *Renewable and Sustainable Energy Reviews*, vol. 211, p. 115333, 2025.

[8] R. E. Alden, C. Halloran, D. D. Lewis, D. M. Ionel, and M. McCulloch, "Assessment of land and renewable energy resource potential for regional power system integration with ml spatio-temporal clustering," in *2023 12th International Conference on Renewable Energy Research and Applications (ICRERA)*. IEEE, 2023.

[9] G. Şahin, A. Koç, and W. van Sark, "Multi-criteria decision making for solar power - wind power plant site selection using a gis-intuitionistic fuzzy-based approach with an application in the netherlands," *Energy Strategy Reviews*, vol. 51, p. 101307, 2024.

[10] G. Demir, M. Riaz, and M. Deveci, "Wind farm site selection using geographic information system and fuzzy decision making model," *Expert Systems with Applications*, p. 124772, 2024.

[11] Y. Yu, X. Han, M. Yang, and J. Yang, "Probabilistic prediction of regional wind power based on spatiotemporal quantile regression," *IEEE Transactions on Industry Applications*, vol. 56, no. 6, 2020.

[12] M. Arrieta-Prieto and K. R. Schell, "Spatio-temporal probabilistic forecasting of wind power for multiple farms: A copula-based hybrid model," *International Journal of Forecasting*, vol. 38, no. 1, 2022.

[13] K. A. Kyeremeh, R. E. Alden, A. Patrick, and D. M. Ionel, "Spatiotemporal wind energy assessment for transmission network integration considering the location of electrical substations and loads," in *2024 13th International Conference on Renewable Energy Research and Applications (ICRERA)*, Nagasaki, Japan, 2024, pp. 1805–1810.

[14] L. Sander, C. Jung, and D. Schindler, "New concept of renewable energy priority zones for efficient onshore wind and solar expansion," *Energy Conversion and Management*, vol. 294, p. 117575, 2023.

[15] Oklahoma Mesonet, "Mesonet wind data," 2023. [Online]. Available: https://www.mesonet.org/weather/wind

[16] J. F. Manwell, J. G. McGowan, and A. L. Togers, *Wind Turbine Siting, System Design, and Integration*. John Wiley Sons, Ltd, 2009, ch. 9.

[17] G. M. Master, *Wind Power Systems*. John Wiley Sons, Ltd, 2004.

[18] Global Modeling and Assimilation Office (GMAO), "MERRA-2 tavg1_2d_slv_Nx: 2d, 1-Hourly, Time-Averaged, Single-Level, Assimilation, Single-Level Diagnostics V5.12.4," Greenbelt, MD, USA, 2015. [Online]. Available: https://doi.org/10.5067/VJAFPLI1CSIV

[19] R. Gelaro, W. McCarty, M. J. Suárez, R. Todling, A. Molod, L. Takács, C. A. Randles, A. Darmenov, M. G. Bosilovich, R. Reichle, K. Wargan, L. Coy, R. Cullather, C. Draper, S. Akella, V. Buchard, A. Conaty, A. da Silva, W. Gu, G. Kim, R. Koster, R. Lucchesi, A. Merkine, and et al., "The modern-era retrospective analysis for research and applications, version 2 (merra-2)," *Journal of Climate*, vol. 30, no. 14, pp. 5419–5454, 2017.

[20] M. Hoogwijk, B. de Vries, and W. Turkenburg, "Assessment of the global and regional geographical, technical and economic potential of onshore wind energy," *Energy Economics*, vol. 26, no. 5, 2004.

[21] J. Dewitz, "National Land Cover Database (NLCD) 2019 Products," 2021. [Online]. Available: https://www.sciencebase.gov/catalog/item/5f21cef582cef313ed940043

[22] A. Danese, M. Garau, A. Sumper, and B. N. Torsæter, "Electrical infrastructure design methodology of dynamic and static charging for heavy and light duty electric vehicles," *Energies*, vol. 14, no. 12, p. 3362, 2021. [Online]. Available: https://doi.org/10.3390/en14123362

[23] E. Ucer, M. Kisacikoglu, A. Gurbuz, S. Rahman, and M. Yuksel, "A machine learning approach for understanding power distribution system congestion," in *2020 IEEE Energy Conversion Congress and Exposition (ECCE)*, 2020, pp. 1977–1983.

[24] M. Kato, Y. Zhou, C. Kang, and R. Yokoyama, "Novel approach of modeling load duration curve for generation expansion planning based on hill's function," *IEEJ Transactions on Electrical and Electronic Engineering*, vol. 6, no. 4, pp. 304–310, Jul. 2011.

[25] C. Crozier, C. Quarton, N. Mansor, D. Pagnano, and I. Llewellyn, "Modelling of the Ability of a Mixed Renewable Generation Electricity System with Storage to Meet Consumer Demand," *Electricity*, vol. 3, no. 1, 2022.

[26] P. Schober, C. Boer, and L. A. Schwarte, "Correlation coefficients: Appropriate use and interpretation," *Anesthesia and Analgesia*, vol. 126, no. 5, pp. 1763–1768, 2018.

[27] A. Phadke, R. Bharvirkar, and J. Khangura, *Reassessing Wind Potential Estimates for India: Economic and Policy Implications*. Carlifornia: Carlifornia Digital Library. [Online]. Available: https://escholarship.org/content/qt7551z3z3/qt7551z3z3.pdf

[28] A. Lopez, A. Levine, J. Carey, and C. Mangan, "U.S. Wind Siting Regulation and Zoning Ordinances (2022)," Open Energy Data Initiative (OEDI), National Renewable Energy Laboratory, https://doi.org/10.25984/1873866, 2022, accessed: 2026-07-01. [Online]. Available: https://data.openei.org/submissions/5733

[29] B. Sliz-Szkliniarz, J. Eberbach, B. Hoffmann, and M. Fortin, "Assessing the cost of onshore wind development scenarios: Modelling of spatial and temporal distribution of wind power for the case of Poland," *Renewable and Sustainable Energy Reviews*, vol. 109, 2019.

[30] U.S. Energy Information Administration, "Electricity Grid Monitor Dashboard: Overview of the U.S.A. Electric Grid," 2024. [Online]. Available: https://www.eia.gov/electricity/gridmonitor/dashboard/electric_overview/US48/US48

[31] Lewis, Donovin D. and Patrick, Aron and Jones, Evan S. and Alden, Rosemary E. and Hadi, Abdullah Al and McCulloch, Malcolm D. and Ionel, Dan M., "Decarbonization analysis for thermal generation and regionally integrated large-scale renewables based on minutely optimal dispatch with a Kentucky case study," *Energies*, vol. 16, no. 4, 2023.

[32] M. Rambabu, R. S. S Nuvvula, P. P. Kumar, K. Mounich, M. E. Loor-Cevallos, and M. Gupta, "Integrating renewable energy and computer science: Innovations and challenges in a sustainable future," in *2023 12th International Conference on Renewable Energy Research and Applications (ICRERA)*, 2023, pp. 472–479.

[33] A. Harrouz, D. Belatrache, K. Boulal, I. Colak, and K. Kayisli, "Social acceptance of renewable energy dedicated to electric production," in *2020 9th International Conference on Renewable Energy Research and Application (ICRERA)*, 2020, pp. 283–288.

[34] Vestas, "4MW Platform Brochure," 2024. [Online]. Available: https://nozebra.ipapercms.dk/Vestas/Communication/4mw-platform-brochure/?page=1

[35] S. Gamesa, "SG 3.4-145 Wind Turbine," 2024. [Online]. Available: https://www.siemensgamesa.com/global/en/home/products-and-services/onshore/wind-turbine-sg-3-4-145.html

[36] A. Eberle, T. Mai, O. Roberts, T. Williams, P. Pinchuk, A. Lopez, M. Mowers, J. Mowers, T. Stehly, and E. Lantz, "Incorporating wind turbine choice in high-resolution geospatial supply curve and capacity expansion models," National Renewable Energy Laboratory, Golden, CO, Tech. Rep. NREL/TP-6A20-87161, 2024.

[37] F. Author and F. Coauthor, "A parametric model for wind turbine power curves incorporating environmental conditions," *Journal of Renewable Energy*, vol. 45, no. 2, pp. 123–134, 2023.

[38] *Wind Turbines – Part 1: Design Requirements*, International Electrotechnical Commission (IEC) Std. IEC 61 400-1, 2019.

[39] AES Corporation, "Delta wind farm," 2024. [Online]. Available: https://www.aes.com/delta-wind-farm

[40] O. M. Akeyo, A. Patrick, and D. M. Ionel, "Study of Renewable Energy Penetration on a Benchmark Generation and Transmission System," *Energies*, vol. 14, no. 1, 2021.

**Kwabena A. Kyeremeh** (Graduate Student Member, IEEE) received the B.Sc. degree in electrical and electronic engineering from the Kwame Nkrumah University of Science and Technology, Ghana, and the M.Sc. degree in electrical engineering from Politecnico di Milano, Italy. He is currently pursuing the Ph.D. degree in electrical engineering with the SPARK Laboratory, Department of Electrical and Computer Engineering, at the University of Kentucky, Lexington, KY, USA.

Prior to his doctoral studies, he served as a Lecturer in electrical engineering at the University of Energy and Natural Resources, Ghana, and as a Research Fellow at the Regional Center for Energy and Environmental Sustainability, Ghana. He also gained industry experience as an Electrical Design Engineer in both Ghana and Germany, contributing to electrical infrastructure and power system projects.

His research focuses on battery energy storage systems, renewable energy integration, power system protection and control, and hardware-in-the-loop testing. His work has been disseminated through peer-reviewed publications and presentations at international conferences

**Rosemary E. Alden** (Member, IEEE) received her B.S. and Ph.D. in electrical engineering from the University of Kentucky (UKY), Lexington, KY in 2021 and 2025, respectively. While at UKY, she was a National Science Foundation (NSF) Graduate Research Fellow, a Pigman undergraduate scholar, a Lighthouse Beacon Foundation Graduate Fellow, and a recipient of IEEE best paper/poster awards. As a PhD student she was also a remote research collaborator and summer visitor with University of Oxford, Oxford, England, UK. She was a researcher on projects supported by major utilities: TVA, LG&E and KU, and PPL, and an intern with the Electric Power Research Institute (EPRI), and the National Renewable Energy Laboratory (NREL). She is currently a research engineer with ABB, Inc. in Raleigh, NC. Her research interests include artificial intelligence, smart home and grid technologies, renewable energy, and electric power systems.

**Aron Patrick** is the Vice President of Research and Development for PPL Corporation responsible for managing an enterprise-wide R&D and strategy across all operating companies including generation, electric and gas delivery, and behind-the-meter opportunities. Aron leads all partnerships with external research organizations, including national laboratories, universities, and the Electric Power Research Institute (EPRI). Aron also coordinates investments from PPL Technology Ventures LLC and venture capital partnerships with Energy Impact Partners (EIP) and The Westly Group venture funds. Before joining PPL in 2016, Patrick held leadership roles at the Kentucky Energy and Environment Cabinet, including assistant director and manager for renewable energy, data analytics, and decarbonization. Prior to joining state government, Aron was an intelligence analyst for the federal government, using statistical analysis and modeling to address national security problems. Aron is a Lexington native, with bachelor's and master's degrees from the University of Kentucky in international commerce, statistics, and political science.

**Dan M. Ionel** (Fellow, IEEE) received the M.Eng. and Ph.D. degrees in electrical engineering from the Polytechnic University of Bucharest, Romania. His doctoral program included a Leverhulme Visiting Fellowship with the University of Bath, England, U.K., and he later was a postdoctoral researcher with the SPEED Laboratory, University of Glasgow, Scotland, U.K.

Dr. Ionel is a professor of electrical engineering and the L. Stanley Pigman Chair in Power with the University of Kentucky, Lexington, KY, USA, where he has been since 2015. He is also the Director of the Power and Energy Institute of Kentucky and of the SPARK Laboratory. In 2024, while on sabbatical, Dr. Ionel was a Leverhulme Visiting Professor in England at University of Bath, expanding also the collaboration with University of Oxford, and was appointed an Honorary Professor at University College London (UCL). He previously worked in industry for more than 20 years, most recently as Chief Engineer/Scientist for large multinational companies.

Dr. Ionel's research group projects on smart grids and buildings, integration of distributed renewable energy resources and energy storage in the electric power systems have been sponsored by NSF, DOE, industry and utilities. He published more than 300 technical papers, including IEEE award winners, was granted more than 40 patents, and is co-author and co-editor of the book "Renewable Energy Devices and Systems – Simulations with MATLAB and ANSYS", CRC Press. Dr. Ionel received the IEEE PES Veinott Award, was the Inaugural Chair of the IEEE IAS Renewable Energy Systems Committee, an editor for journals, and chair for large international conferences.